Electrochemistry

International Edition: DOI: 10.1002/anie.201708735
German Edition: DOI: 10.1002/ange.201708735

The van der Waals Interactions of *n*-Alkanethiol-Covered Surfaces: From Planar to Curved Surfaces

Fernando P. Cometto, Zhi Luo, Shun Zhao, Jimena A. Olmos-Asar, Marcelo M. Mariscal, Quy Ong, Klaus Kern, Francesco Stellacci, and Magalí Lingenfelder**

Abstract: *The van der Waals (vdW) interactions of n-alkanethiols (ATs) adsorbed on planar Au(111) and Au(100) surfaces and curved Au nanoparticles of different diameters are reported. By means of electrochemical measurements and molecular dynamic calculations, the increase in the average geometrical curvature of the surface influences the global interactions, that is, decreasing vdW interactions between neighboring molecules. Small NPs do not present the same electrochemical behavior as planar surfaces. The transition between nanoparticle to flat surface electrochemical response is estimated to occur at a circa 13–20 nm diameter range.*

Monolayer-protected nanoparticles (MPNPs) have attracted the attention of many research teams around the world for their potential use in for example medicine, cosmetics, and drug delivery.[1–3] Nevertheless, a full understanding of their structure and behavior remains elusive. The combination of several experimental techniques together with the aid of computer simulations offers the possibility of obtaining a comprehensive picture of these nanostructured systems.

MPNPs can be described as being composed of four different parts: a metal core NP, a head-group that binds to the metal surface through covalent, noncovalent, or ionic interactions; a spacer part, which makes up the interphase between the metal core and the medium; and finally, a terminal group that is in direct contact with the environment. The head group or linker determines the strength of the interaction between the molecule and the metal. Very recently, it has been shown how the head-group–metal interaction affects the crystalline structure of MPNPs.[4] In particular, significant surface damage is observed in AuNPs passivated by thiol molecules, whereas soft ligands (for example $-NH_2R$) do not produce almost any distortion in the crystalline structure of metallic NPs.

The spacer chains of adjacent molecules interact via van der Waals and/or ionic interactions and confer stability to the adsorbed monolayer. If molecules interact strongly, the monolayer will be well packed and the nanoparticle will be more protected.[5,6] The tail or terminal group can be chosen for functionalizing the nanoparticle. It determines the properties of the outer layer, tuning its interactions with the environment. For example, affinity with the media can be managed through some groups, such as $-NH_2$, $-COOH$, or $-OH$ that make the system hydrophilic and $-CH_3$ or $-CF_3$ that turns the system hydrophobic. The possibility of choosing the terminal group of molecules in such a way that they can selectively bind to specific targets is an important challenge for medical and technological applications.

The intermolecular interactions between ligands once adsorbed on the NPs are of key importance because, together with the S–Au binding energy, they determine the stability of the covered surfaces.[5] In this work, we measure the reductive desorption (RD) of *n*-alkanethiols (ATs) with different chain length adsorbed on planar single crystal gold surfaces (Au(111) and Au(100)) and on gold NPs of various diameters. The analysis of the electrochemical data help us to elucidate how vdW interactions between adjacent adsorbed ATs decrease according to the geometrical curvature of the surface. The dependence of vdW interactions on the curvature of the surface is in agreement with molecular dynamics calculations.

Figure 1a shows cyclic voltammograms (CV) displaying the RD of ATs of different chain length (C6, C9, C12) in alkaline medium from Au (111), Au (100) planar surfaces, 3 nm and 5 nm AuNPs deposited on highly ordered pyrolytic graphite (HOPG), whereas Figure 1b shows the desorption peak potential of the RD vs. the chain length (number of carbon atoms in the aliphatic chain). Given a simplified electroreductive equation for ATs adsorbed on a Au surface:[7,8]

$$RS{-}Au + e^- \rightarrow RS^- + Au \quad (1)$$

it is possible to obtain the surface coverage of ATs on Au by the integration of the reductive peak (the area of the peak is related to the number of molecules desorbed per unit area). The position of the desorption peak in the RD process can be considered as a measure of the electrochemical stability of the

[*] Dr. F. P. Cometto, Prof. Dr. K. Kern, Dr. M. Lingenfelder
Max Planck-EPFL Laboratory for Molecular Nanoscience, and Institut de Physique, École Polytechnique Fédérale de Lausanne
1015 Lausanne (Switzerland)
E-mail: fernando.cometto@epfl.ch
magali.lingenfelder@epfl.ch
Dr. F. P. Cometto, Dr. J. A. Olmos-Asar, Dr. M. M. Mariscal
Departamento Fisicoquímica y de Química Teórica y Computacional, Facultad de Ciencias Químicas, Universidad Nacional de Córdoba—INFIQC, Instituto de Investigaciones en Fisicoquímica de Córdoba, CONICET (Argentina)
Z. Luo, S. Zhao, Dr. Q. Ong, Prof. Dr. F. Stellacci
Institute of Materials, École Polytechnique Fédérale de Lausanne
Lausanne 1015 (Switzerland)
Prof. Dr. K. Kern
Max-Planck-Institut für Festkörperforschung
70569 Stuttgart (Germany)
Supporting information and the ORCID identification number(s) for the author(s) of this article can be found under: https://doi.org/10.1002/anie.201708735.

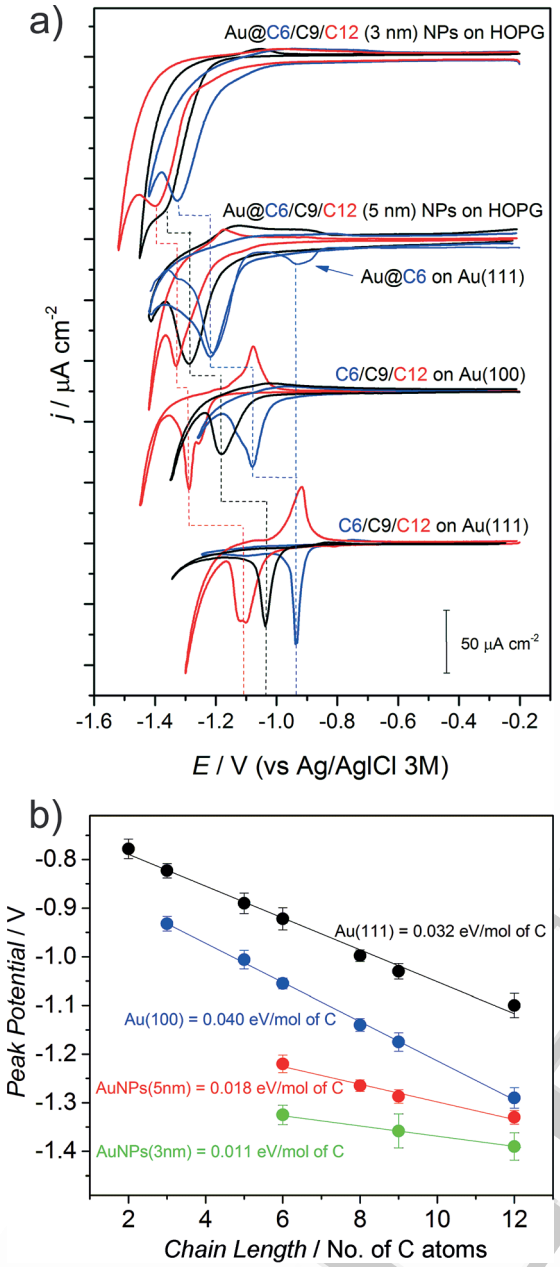

Figure 1. a) Cyclic voltammograms showing the RD of ATs on Au (111), Au (100), 3 nm NPs, and 5 nm NPs.■■ok?■■ Electrolyte: KOH 0.1 M. Scan rate: 50 mV s^{-1}. b) Peak potential vs. chain length obtained after RD. Lines represent the linear regression for every substrate.

SAM, reflecting a global free energy change between the initial and final states. Doneux et al.[9] proposed a more realistic description for the reductive desorption process:[9–11]

$$RS_{(surface,Au(hkl))} + x\,H_2O_{(aq)} + n\,e^-_{Au(hkl)} \rightleftharpoons RS^-_{(aq)} + x\,H_2O_{(surface,Au(hkl))} \quad (2)$$

instead of the simplified Equation (1), where the aggregation state of every species is defined specifically.[9] Thus, the energetic contributions that should be considered are the following: 1) substrate–adsorbate interaction (Au(*hkl*)–S; determined by the head-group/surface binding energy); 2) lateral interactions (C_n/vdW$_{Au(hkl)}$; mainly attractive vdW forces that contribute to stabilise the monolayer, shifting the RD potential towards more negative values);[12,13] 3) substrate/SAM–solvent (potential of zero charge of thiol-solvent interactions in the adsorbed state, pzc$_{CnT\text{-}Au(hkl)}$); 4) desorbed surfactant–solvent (C_n/solvent; AT solvation energy); and 5) substrate–solvent, (pzc$_{bare\ Au(hkl)}$; directly dependent on the difference between the applied potential and the pzc of the bare gold surface).[9] The contributions 1–3 are attributed to the initial state of the process described in Equation (2), whereas 4–5 are to the final state. Therefore, the RD potential peak depends on:

$$E_p([Au(hkl)/S];\ [C_n/vdW_{Au(hkl)}];\ [pzc_{CnT-Au(hkl)}];\ [C_n/solvent];\ [pzc_{bare\ Au(hkl)}]) \quad (3)$$

The electroreductive desorption technique has been used mostly on Au (111) surfaces.[14] For the case of *n*-alkanethiols, the peak area is considered not to change with the chain length if a complete AT monolayer is desorbed from the surface[15] [Eq. (1)]. Nevertheless, it is expected that the position of the desorption potential changes according to the chain length [Eq. (3)], that is, longer ATs are desorbed at more negative values. In other words, whereas Au(111)–S and pzc$_{bare\ Au(111)}$ remain constant for the desorption of ATs of different length from a specific substrate (Au(111)), the lateral interactions (C_n/vdW$_{Au(111)}$) and the surfactant–solvent interactions (C_n/solvent), change.■■ok?■■ Therefore, the desorption potential shifts to more negative values with an increase in the chain length.[16]

Here we show that the same trend is observed for ATs adsorbed on Au(100) and AuNPs (Figure 1 a). The desorption potential values are shifted to more negative values from that of Au(111). Salvarezza et al.[17] showed a similar behavior for AuNPs compared to AT desorption from nanostructured rough gold electrodes.

Masens et al.[18] reported by theoretical calculations that the binding energy of thiolates on more open surfaces, such as Au (100) and Au (110), are larger than on Au (111) by about 10 kcal mol^{-1}. This tendency was also observed by Cortés et al[19] for nanostructured gold substrates.

Accordingly, electrochemical characterization of ATs adsorbed on different gold surfaces[20–22] reported that shifts in the RD peaks correlate with binding strengths on different facets of crystalline gold surfaces and are also related to the pzc of the bare crystals, which is different for every facet.[9,21] Considering that for AuNPs greater than 3 nm, about 1/3 of the surface is composed of 100 planes and about 2/3 by 111 planes,[23] earlier works[24–26] hypothesized that each desorption peak obtained for thiol-covered AuNPs should be associated to different S–Au binding strengths arising from different facets and facet boundaries. Rahman et al.[26] measured the RD of cysteine molecules covering 25 nm AuNPs deposited on glassy carbon. They obtained two well-defined desorption peaks that according to an earlier work of the same group[20] correlate very well with the desorption profiles of cysteine molecules from Au(111) and Au(100), respectively. In contrast with previous works,[24–26] we observe

a single peak for the desorption process of smaller NPs (3 and 5 nm NPs on HOPG (Figure 1a). For 5 nm Au@C6 NPs, we only found two peaks when the deposition of NPs was made during 24 h on a Au(111) substrate (Au@C6 on Au(111) in Figure 1a). In this case, one peak is attributed to the desorption of C6 from NPs (the peak coincides with that observed for the RD of the same NPs deposited on HOPG and is independent of the scan rate) and the second peak from planar 111 Au surfaces. The presence of C6 molecules on the planar surfaces could be attributed to ligand exchange of molecules from the NPs to the planar surface.

The RD potential of ATs adsorbed on Au (100) is shifted to more negative values compared with the desorption potential of Au (111) (Figure 1a). The double peak shown for C12 on every crystalline facet is attributed to the fine structure in the voltammetric waves for alkyl chains of more than 10 carbons.[27] Surprisingly, it is observed that the desorption potential from 3 and 5 nm AuNPs does not coincide neither with the desorption potential from Au (111) nor from Au (100) facets.[26,23] This indicates that the increased binding energy of ATs on the gold curved surface of small NPs could be associated to an overall restructuring of the NP after adsorption (by means of adatoms, staple-motif or surface disorder)[28] creating a homogeneous ligand shell. The desorption of this shell is therefore different than the desorption of thiols from crystalline facets on larger gold NPs.[23] These findings indicate that the particle size should play a key role in the determination of the surface reconstruction upon ATs adsorption. If the size of the NP is large enough, the NP interface properties might approximate to those of planar surfaces,[23] as we shall describe for larger NPs.

It is interesting to note that RD technique can also be used to determine size selectivity; for smaller NPs (as in the case of 3 nm NPs), the RD potential shifts to more negative values. In the Supporting Information, Figure S3a, we measure the RD of a polydisperse sample containing different populations, and we found that every population correlates very well with RD potentials associated with specific NP sizes. As surfactant–solvent interactions are the same for any specific AT and, as we shall see, lateral interactions decrease in smaller NPs, mostly the Au(x nm)–S (and solvent–bare-substrate ($pzc_{bare\ Au(x\ nm)}$)) interactions are responsible for the shift in the RD potential to more negative values. Thus, the shift to more negative values, in this case, should be mainly related to an increase in the binding energy of the S head group to the gold surface atoms and changes in the pzc of the bare NPs.

Whereas the S–Au binding energy of the ATs on NPs increases as the NP size decreases, Murray et al.[29] suggested a decrease in the chain packing density for high curvature gold nanoparticle surfaces. Therefore, it should be reasonable that vdW interactions decrease for curved surfaces. Figure 1b shows the straight lines obtained after fitting the reductive potential values vs. chain length (number of carbon atoms in the aliphatic chain) for different planar surfaces and NPs. For the Au(111) surface a slope value ($S_{Au(111)}$) of 0.032 eV per mol of C atom is obtained, in agreement with previous works.[15,30,31] The slope value ($S_{Au(hkl)}$) obtained from different chain length (n) of ATs adsorbed on the same surface Au(hkl), would only depend on:

$$S_{Au(hkl)} = ([C_{n+1}/\text{solvent}]-[C_n/\text{solvent}]; [pzc_{C(n+1)T-Au(hkl)}]-[pzc_{CnT-Au(hkl)}]; [C_{n+1}/vdW_{Au(hkl)}]-[C_n/vdW_{Au(hkl)}]) \quad (4)$$

because the Au(hkl)–S interaction and the solvent-surface interactions after desorption ($pzc_{bare\ Au(hkl)}$) do not depend on the chain length. Thus, the $S_{Au(111)}$ should only be proportional to the change in the *vdW* interactions and hydrophobic forces per methylene group (C_{n+1}–C_n).

If the same analysis is made for a different surface (Au($h'k'l'$)), the new slope value $S_{Au(h'k'l')}$ would also be proportional to the change in the lateral interactions and hydrophobic forces per methylene group (C_{n+1}–C_n) for the new trial surface. If we take the subtraction of the corresponding slopes of two different facets:

$$S_{Au(hkl)}-S_{Au(h'k'l')} = ([C_{n+1}vdW_{Au(hkl)}]-[C_nvdW_{Au(hkl)}])-([C_{n+1}vdW_{Au(h'k'l')}]-[C_nvdW_{Au(h'k'l')}]) \quad (5)$$

it would only account for the change in vdW interactions per methylene group comparing two different surfaces; because $[C_{n+1}T-\text{solvent}]-[C_nT-\text{solvent}]$ and $[pzc_{CnT-Au(hkl)}]-[pzc_{CnT-Au(h'k'l')}]$ terms hardly depend on the surface crystallinity. That is, because the same surfactants are compared for different surfaces, a change in the slope value would only account for lateral interactions between neighbor adsorbates in the initial state of the reductive desorption process.

Thus, if we compare the slope value obtained from the slope for planar Au(111) ($S_{Au(111)} = 0.032\ eV\,mol^{-1}$) from that obtained for AuNPs ($S_{Au(5\ nm)} = 0.018\ eV\,mol^{-1}$, $S_{Au(3\ nm)} = 0.011\ eV\,mol^{-1}$), we obtain a decrease in the *vdW* interactions of $0.014\ eV\,mol^{-1}$ and $0.021\ eV\,mol^{-1}$ per C atom from planar Au(111) to 5 nm and 3 nm curved surfaces, respectively. The vdW energy decrease (compared to a fully covered 111 planar surface) versus the NP size obtained by EC data, is shown in Figure 2 (red points).

Molecular dynamic (MD) calculations have been performed to gain knowledge on the vdW interactions between neighboring AT molecules on curved surfaces. Figure 2 shows the decrease of the vdW interactions obtained by MD (blue triangles) and EC data (red points) obtained above. Intermolecular interactions have been obtained performing MD calculations for AuNPs with truncated octahedral shape of four different diameters; 1.8, 2.7, 3.8, and 4.2 nm (201, 586, 1291, and 2406 gold atoms; respectively) and for a planar 111 surface. Each surface is fully covered by n-heptanethiolate (C7) species. VdW interactions have been calculated by normalizing the total energy for the number of molecules and then divided by 7 carbon atoms. Fixing the value of the intermolecular interactions of the planar surfaces to zero (subtracting *vdW* interactions when $R \to \infty$), we obtain how these interactions decrease with the geometrical curvature of the surface (Figure 2, blue triangles).

Following the theoretical points, an optimized trend that behaves as an attractive Lennard-Jones-type potential was obtained from a simple model (see the Supporting Information). Therefore, the decrease of the vdW interactions (blue

Dateiname: Z708735e
Pfad: l:/daten/verlage/vch/ach/hefte/pool/
Status Neusatz
Datum: 46 KW., 13. November 2017 (Montag)
Pagina: 3
Seite: 3 te von 6
Umfang (Seiten): 6
Zeit: 6:08:47 Uhr

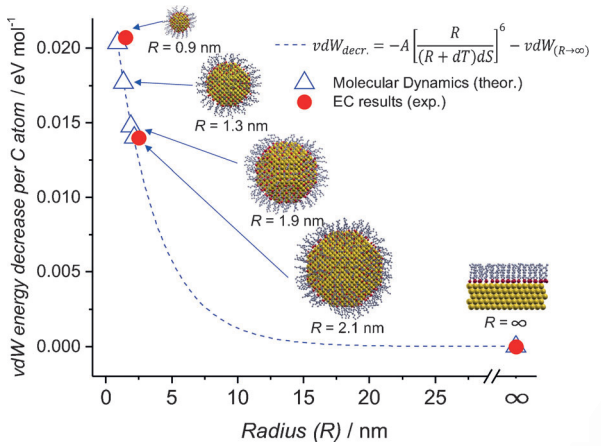

Figure 2. vdW energy decrease obtained by molecular dynamic calculations (blue triangles) and EC results (red points; 3 nm, 5 nm, and Au(111)) versus the radius (R) of NPs. The dashed blue line represents the optimized trend that behaves as an attractive Lennard-Jones-type potential obtained from the theoretical points, where R is the NP radius, dT is the length of the thiol, and dS is a function that depends both on R and the arc length between thiols. The parameters for the vdW decrease are: $A = 3.98 \times 10^{-5}$ eV nm^6 mol^{-1}; dT = 0.88 nm and dS = 0.3 nm.

dotted line) with the radius (R) of the NPs was obtained after the subtraction of the vdW energy when $R \rightarrow \infty$; where a good agreement with the experimental measurements is observed for 3 and 5 nm AuNPs (Figure 2, red points). From this trend, it can be also noticed that there should be a transition in the nanoparticle behavior in the 13–20 nm diameter range; that is, for bigger NPs vdW interactions are quite similar to those obtained on planar surfaces, in agreement with the shifts on the RD peaks observed for larger nanoparticles.[26]

The desorption potential vs. the diameter of the NPs for electrochemical measurements with C6, C8, C9, and C12 covered AuNPs of different sizes, shows that the desorption potential becomes more negative as the diameter of the NPs decreases (preserving for each size, a chain length dependence; Supporting Information, Figure S3 b). A detailed experimental analysis of larger NPs is not straightforward. Since small *n*-alkanethiol covered AuNPs are synthetized by a known direct method where NPs were dissolved in an organic solvent (such as dichloromethane or toluene),[32]■■[32] instead of [33]: ok?■■ the same procedure fails in the synthesis of larger AT-covered AuNPs due to precipitation. To overcome this problem, larger NPs were synthetized by an indirect method: first AuNPs of 13, 20 nm and 100 nm were prepared in an aqueous solution (NPs covered by citrates) and then by ligand exchange, the corresponding ATs adsorb on the NPs. The main difference with the direct method is that the ATs density should be lower and a decrease in the vdW interactions between neighbors should be appreciable. This fact is used to validate the strength of the RD technique in the determination of the energetic contribution of the ligands on NPs.

Cathodic sweeps showing the RD of C6, C9, and C12 from 13 nm, 20 nm, and 100 nm AuNPs, are shown in Figure 3 a). The analysis of the RD potentials vs. chain length showing

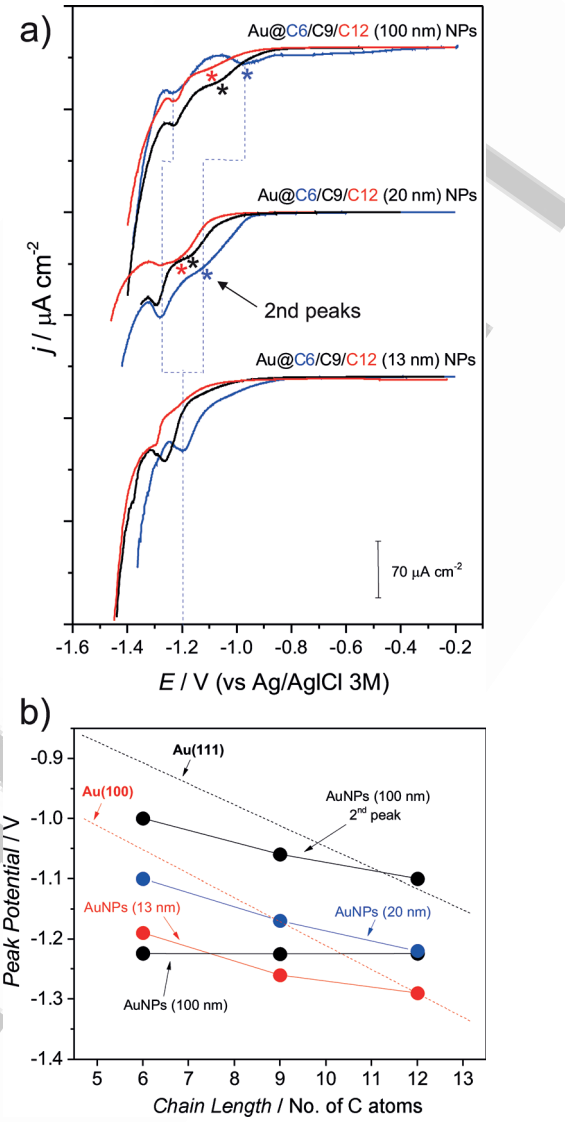

Figure 3. a) Cathodic sweeps showing the RD of ATs on 13 nm, 20 nm, and 100 nm AuNPs. Electrolyte: KOH 0.1 M. Scan rate: 50 mV s^{-1}. b) Peak potential vs. chain length obtained after RD. For clarity, slopes representing the Au(111) and Au(100) chain length dependence are included.

a decrease in the vdW interactions (decrease of the slope RD potential vs. number of C atoms) are presented in Figures 3 b (see the Supporting Information, Figure S4 for details).■■ok?■■ In the case of 13 nm AuNPs, a single RD peak is obtained and the expected chain-length dependence is observed; that is, RD peaks shift to more negative values with an increase in the length of the ATs. The slope obtained after the linear regression of RD potential vs. the number of C atoms is almost the same value obtained for 5 nm AuNPs (0.017 vs. 0.018 eV mol^{-1} of C atoms). According to our hypothesis and the trend line accounting to the decrease in the vdW interactions with the curvature from MD calculations, we expected a value closer to the slope obtained for the 111 planar surface (closer to zero in Figure 2)). We attribute this, to the ligand exchange synthesis, where the NPs obtained have lower ligand density and thus, vdW interactions are

underestimated (Supporting Information, Figure S4). Further evidence provided for bigger NPs (13, 20, and 100 nm) demonstrates our previous prediction: two broad peaks appear in the cathodic sweeps (Figure 3a) in the region of the RD potentials obtained for 111 and 100 that could be associated to desorption from different facets of the NPs. In both cases (20 nm and 100 nm NPs) is noticeable that the more negative peak is almost independent of the chain length (Figure 3a,b) showing similar influence of the vdW interactions between neighbors (typical behavior of poorly dense-packed submonolayers). In the case of 100 nm NPs, the second peak almost coincide with the 111 planar surface, but showing a decrease in the vdW interactions due to the lower ligand density (Figure 3b). In conclusion, we use electrochemical measurements to determine how the nature of the chemical bonds (specifically ATs on gold) changes with different surfaces; from single crystals, such as Au (111) and Au (100), to spherical AuNPs of different diameters. We find that small NPs do not present the same electrochemical behavior obtained for planar surfaces. Furthermore, we show how vdW interactions decrease with the geometrical curvature of the surface. This finding is corroborated by MD calculations that led us to propose the existence of a transition between nano- to macroscale behavior at the circa 13–20 nm size regime. Also, we validate the RD technique showing energetic deviations according to the ligand density on larger NPs. The present work emphasizes the need to clarify the chemical nature of ATs on different surfaces. To this end, further theoretical and experimental work should include RD measurements of different chain length ATs from NPs of different geometries, such as gold nanorods (AuNRs) with different minor/major axis ratio to study the RD of thiols from different ratios of 111 and 100 facets.

Acknowledgements

We thank the MPI-EPFL Center for financial support. F.P.C. and M.L. thanks Prof. S. Dassie and Prof. K. Balasubramanian for fruitful discussions. J.A.O.A. and M.M.M. thank CONICET, ANPCyT Mincyt PICT 2191/2015 and UNC for financial support. F.S. and Z.L. thank the Swiss National Science Foundation for support.

Conflict of interest

The authors declare no conflict of interest.

Keywords: alkanethiols · electrochemistry · gold nanoparticles · molecular dynamic simulations · van der Waals interactions

[1] X. Liu, M. Yu, H. Kim, M. Mameli, F. Stellacci, *Nat. Commun.* **2012**, *3*, 1182.
[2] R. C. Van Lehn, A. Alexander-Katz, *J. Phys. Chem. C* **2013**, *117*, 20104 – 20115.
[3] M. M. Mariscal, O. A. Oviedo, E. P. M. Leiva, *Metal Clusters and Nanoalloys*, Springer New York, New York, **2013**.
[4] J. A. Olmos-Asar, M. Ludueña, M. M. Mariscal, *Phys. Chem. Chem. Phys.* **2014**, *16*, 15979 – 15987.
[5] F. Schreiber, *J. Phys. Condens. Matter* **2004**, *16*, R881.
[6] A. Ulman, *Chem. Rev.* **1996**, *96*, 1533 – 1554.
[7] M. M. Walczak, D. D. Popenoe, R. S. Deinhammer, B. D. Lamp, C. Chung, M. D. Porter, *Langmuir* **1991**, *7*, 2687 – 2693.
[8] C. A. Widrig, C. Chung, M. D. Porter, *J. Electroanal. Chem. Interfacial Electrochem.* **1991**, *310*, 335 – 359.
[9] T. Doneux, M. Steichen, A. De Rache, C. Buess-Herman, *J. Electroanal. Chem.* **2010**, *649*, 164 – 170.
[10] J. Kunze, J. Leitch, A. L. Schwan, R. J. Faragher, R. Naumann, S. Schiller, W. Knoll, J. R. Dutcher, J. Lipkowski, *Langmuir* **2006**, *22*, 5509 – 5519.
[11] T. Laredo, J. Leitch, M. Chen, I. J. Burgess, J. R. Dutcher, J. Lipkowski, *Langmuir* **2007**, *23*, 6205 – 6211.
[12] F. P. Cometto, C. A. Calderón, M. Berdakin, P. Paredes-Olivera, V. A. Macagno, E. M. Patrito, *Electrochim. Acta* **2012**, *61*, 132 – 139.
[13] M. E. Vela, H. Martin, C. Vericat, G. Andreasen, A. Hernández Creus, R. C. Salvarezza, *J. Phys. Chem. B* **2000**, *104*, 11878 – 11882.
[14] T. Kakiuchi, H. Usui, D. Hobara, M. Yamamoto, *Langmuir* **2002**, *18*, 5231 – 5238.
[15] O. Azzaroni, M. E. Vela, H. Martin, A. Hernández Creus, G. Andreasen, R. C. Salvarezza, *Langmuir* **2001**, *17*, 6647 – 6654.
[16] See Ref. [13].■■ok?■■
[17] D. Grumelli, C. Vericat, G. Benitez, M. E. Vela, R. C. Salvarezza, L. J. Giovanetti, J. M. Ramallo-López, F. G. Requejo, A. F. Craievich, Y. S. Shon, *J. Phys. Chem. C* **2007**, *111*, 7179 – 7184.
[18] C. Masens, M. J. Ford, M. B. Cortie, *Surf. Sci.* **2005**, *580*, 19 – 29.
[19] E. Cortés, A. A. Rubert, G. Benitez, P. Carro, M. E. Vela, R. C. Salvarezza, *Langmuir* **2009**, *25*, 5661 – 5666.
[20] K. Arihara, T. Ariga, N. Takashima, K. Arihara, T. Okajima, F. Kitamura, K. Tokuda, T. Ohsaka, *Phys. Chem. Chem. Phys.* **2003**, *5*, 3758 – 3761.
[21] D.-F. Yang, C. P. Wilde, M. Morin, *Langmuir* **1996**, *12*, 6570 – 6577.
[22] C.-J. Zhong, J. Zak, M. D. Porter, *J. Electroanal. Chem.* **1997**, *421*, 9 – 13.
[23] J. C. Azcárate, G. Corthey, E. Pensa, C. Vericat, M. H. Fonticelli, R. C. Salvarezza, P. Carro, *J. Phys. Chem. Lett.* **2013**, *4*, 3127 – 3138.
[24] F. L. Leibowitz, W. Zheng, M. M. Maye, C.-J. Zhong, *Anal. Chem.* **1999**, *71*, 5076 – 5083.
[25] C. J. Zhong, W. X. Zheng, F. L. Leibowitz, *Electrochem. Commun.* **1999**, *1*, 72 – 77.
[26] M. R. Rahman, F. S. Saleh, T. Okajima, T. Ohsaka, *Langmuir* **2011**, *27*, 5126 – 5135.
[27] C.-J. Zhong, M. D. Porter, *J. Electroanal. Chem.* **1997**, *425*, 147 – 153.
[28] H. Häkkinen, *Nat. Chem.* **2012**, *4*, 443 – 455.
[29] A. C. Templeton, M. J. Hostetler, C. T. Kraft, R. W. Murray, *J. Am. Chem. Soc.* **1998**, *120*, 1906 – 1911.
[30] M. M. Walczak, C. A. Alves, B. D. Lamp, M. D. Porter, *J. Electroanal. Chem.* **1995**, *396*, 103 – 114.
[31] D. W. Hatchett, R. H. Uibel, K. J. Stevenson, J. M. Harris, H. S. White, *J. Am. Chem. Soc.* **1998**, *120*, 1062 – 1069.
[32] N. Zheng, J. Fan, G. D. Stucky, *J. Am. Chem. Soc.* **2006**, *128*, 6550 – 6551.

Manuscript received: August 24, 2017
Revised manuscript received: October 16, 2017
Accepted manuscript online: October 24, 2017
Version of record online: ■■ ■■, ■■■■

Communications

Electrochemistry

F. P. Cometto,* Z. Luo, S. Zhao, J. A. Olmos-Asar, M. M. Mariscal, Q. Ong, K. Kern, F. Stellacci, M. Lingenfelder* _____ ■■■■–■■■■

The van der Waals Interactions of *n*-Alkanethiol-Covered Surfaces: From Planar to Curved Surfaces

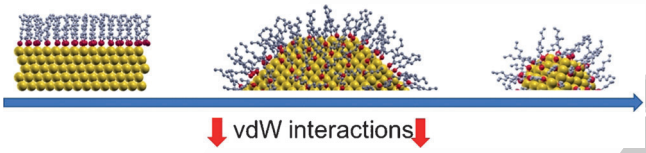

From planar to curved surfaces: The way that the geometrical curvature of the surface influences the global van der Waals interactions between thiol molecules is visualized by means of electrochemical measurements and molecular dynamic calculations.

Elektrochemie

F. P. Cometto,* Z. Luo, S. Zhao, J. A. Olmos-Asar, M. M. Mariscal, Q. Ong, K. Kern, F. Stellacci, M. Lingenfelder* _____ ■■■■–■■■■

The van der Waals Interactions of *n*-Alkanethiol-Covered Surfaces: From Planar to Curved Surfaces

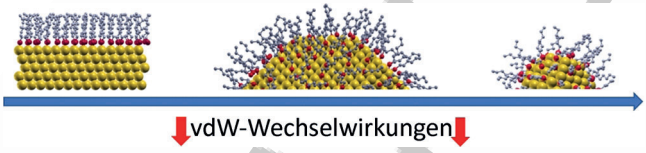

Von planaren zu gekrümmten Oberflächen: Die Art, in der die geometrische Krümmung der Oberfläche die globalen Van-der-Waals-Wechselwirkungen zwischen Thiolmolekülen beeinflussen, wird mit elektrochemischen Messungen und Molekulardynamiksimulationen untersucht.

Please check that the ORCID identifiers listed below are correct. We encourage all authors to provide an ORCID identifier for each coauthor. ORCID is a registry that provides researchers with a unique digital identifier. Some funding agencies recommend or even require the inclusion of ORCID IDs in all published articles, and authors should consult their funding agency guidelines for details. Registration is easy and free; for further information, see http://orcid.org/.

Dr. Fernando P. Cometto
Zhi Luo
Shun Zhao
Dr. Jimena A. Olmos-Asar
Dr. Marcelo M. Mariscal
Dr. Quy Ong
Prof. Dr. Klaus Kern
Prof. Dr. Francesco Stellacci
Dr. Magalí Lingenfelder http://orcid.org/0000-0003-1362-8879